Malaysian
Journal Of Civil
Engineering

CORRELATION BETWEEN INTENSITY MEASURE PARAMETERS OF GROUND MOTION EARTHQUAKES AND STRUCTURAL RESPONSE OF MOMENT RESISTING STEEL FRAMES

Emad Ali Elhout*

Construction Engineering and Management Department, faculty of engineering, Pharos University in Alexandria, Canal Mahmoudiah Street, Ezbet El-Nozha, Sidi Gaber, Alexandria, Egypt

Article history
Received
14 March 2020
Received in revised form
9 September 2020
Accepted
13 September 2020
Published online
30 November 2020

*Corresponding author
emad.elhout@pua.edu.eg

Abstract

Identify and select a suitable ground motion intensity measure (IMs) parameters associated with the structural response to specific levels of damages or collapse in structures are very important in the seismic response of structural analyses. This paper investigated the correlation between 25 intensity measure (IMs) parameters of earthquakes and the structural response parameters of 3-, 6- and 12-story moment resisting steel frames (MRSFs). Nonlinear time history analyses are performed for these frames under near- and far-source ground motion records. The maximum story drift ratio (MSDR), the roof drift ratio (RDR), and the maximum base shear force (SF) are chosen as the structural response parameters. The Pearson correlation coefficient with the regression analyses is utilized to display the correlation between the structural response parameter and the ground motion IMs parameters. The results reveal that MSDR appears to be a suitable engineering demand parameter to correlate with most of the ground motion IMs parameters compared to both the RDR and the SF parameters. Also, Max. Incremental velocity (MIV) parameter is considered as the highest correlated IMs parameters with MSDR in both near- and far-source earthquakes.

Keywords: *Intensity measure parameters, seismic response of structures, Near-source, Far-source, nonlinear time history analysis*

1.0 INTRODUCTION

The main objective of the seismic engineering design is to achieve the life safety and prevent the collapse of the structure. However, until now, the risk of structural failure has not been identified. Determining the risk of collapsing structures depend on their behavior and the site of seismic hazard. The seismic hazard levels are described by using ground motion IMs parameters while the structure behavior is defined by the nonlinear time history analysis. So, it is important to identify and select a suitable ground motion IMs parameter associated with the structural response to design and evaluate the performance of new and existing structures, especially in the active seismic zones. Once the perfect IMs is selected, then the performance of the structures can be evaluated by determining their exposure to specific levels of damages or to collapse.

The correlation between ground motion IMs and seismic structural response parameters has been investigated by many researchers. Markis and Black, (2004) indicating that in both linear and nonlinear structural responses the peak pulse acceleration IM is more demonstrative than the peak pulse velocity for near-fault earthquakes. Riddell (2007) investigated the correlations between 23 ground motion intensity indices with response variables. These variables are elastic, inelastic deformation demands, hysteretic energy, and input energy. The results indicated that the PGA, PGV, and PGD presented an excellent correlation in elastic and inelastic response variables. Also, the best index correlated in the velocity region with both spectral ordinates and energy responses is the Housner's intensity.

The relating between magnitude and epi-central distance earthquake parameters with damage prediction equation is proposed by Hancock et al. (2008). Yang et al. (2009) studied the relationship between different IMs of near-fault ground motion records and the maximum inelastic displacements of a SDOF structure. The results indicated that the peak ground acceleration (PGA) is the best IM parameter for systems of short-period. Also, peak ground velocity (PGV) and peak ground displacement (PGD) are the particular ground motion IMs parameters for systems of medium and long-period. Perrault and Guéguen (2015) studied the relationship between building response and IMs, such as PGA, PGV, Sd, and CAV. Different types and heights of steel and RC building structures are used in the analysis. The normalized relative roof displacement is considered as the predictability of building response. Also, an empirical model for damage prediction equation based on IMs is proposed. Habibi and Jami (2016) determined the relationship between IM parameters of far-field earthquakes and the target displacement (T_D) of 3- and 9-story steel frames. The analysis indicated that HI, SA, SV, and PGV exhibit the strongest correlated while PGA is the weakest correlated parameter with T_D.

Shokrabadi and Burton (2017) evaluated the effect of ground motion IMs (PGA, Sa (T1), Sa_{avg} and S_{di}) in predicting story drift ratio, peak floor acceleration, and residual story drift ratio for two types of rocking building systems. 37 records of near- and far-field ground motions are used in this study. Sa_{avg} is the most real parameter for expecting transient and residual drift demands while PGA is the best predictor parameter of peak floor accelerations. Kenari and Celikag (2019) evaluated the correlation between different IMs parameters of ground motion and damage parameters in 3-, 5-, 8- and 12-story steel structures. Ordinary (OSR) and pulse-like seismic records (PLSR) earthquake ground motions with the Open SEES program are used in nonlinear time history analysis. The analysis shows that EPV, VSI, and HI have the highest correlation with the MIDR in both OSR and PLSR category. Esfahanian and Aghakouchak (2020) investigated the effect of intensity levels of near- and far-fault ground motion on the seismic behavior of two moment resisting steel frames. The roof displacement and inter-story drift are used as seismic demands. These results indicated that the story drifts for near-fault motions in the lower story levels are larger than that for far-fault records. Pinzon et al. (2020) investigated the correlation between IMs of forty pairs of strong ground motion from the Italian database and the MSDR of 3-, 7- and 13-story steel structures. The results indicate that the worst correlation is between PGA and MIDR show. PGV, root-mean-square velocity, and specific energy density intensity-based measures are the higher correlation.

Previous studies are depending on a limit of IMs parameters and did not consider the effect of building heights. This study investigated the correlation between different IMs parameters of near- and far-source ground motions with structural response parameters of 3-, 6- and 12-story MRSFs. The IMs parameters that consider in this study such as peak ground acceleration (PGA), velocity (PGV), displacement (PGD), PGA/PGV ratio, arias intensity (Ia), Housner intensity (HI), cumulative absolute velocity (CAV), A95 parameter, The predominant period (T_p), the mean period (T_m), the number of effective cycles (N_{cy}), The damage index (DI), the impulsivity index (IP), the average spectral acceleration (SA_{avg}). The structural response parameters were expressed in terms of the MSDR, RDR, and SF as recommended by Jayaram (2010).

2.0 STRONG MOTION DATABASE AND INTENSITY MEASUREMENT PARAMETERS

Near- and far-source ground motion records identified by FEMA P695 (2009) are used in this study. FEMA P695 (2009) took near-source ground motion records for source to site distance less or equal 10 km and far-source for greater than 10 km. The site source distances are given in several different measures such as epicentral, the closest to plane, Campbell, and Joyner-Boore distance. The average of Campbell and Joyner-Boore fault distances was taken as the source to site distance in the PEER NGA database. These ground motions are consisting of 49 acceleration records (each with two horizontal components) with a variety of characteristics. The characteristics of near-field records are the moment magnitudes (M6.5 - M7.9), the average of Campbell and Boore-Joyner fault distances, (1.7-8.8 km), and site class (B, C, and D) as shown in table 1. For far-field records, the moment magnitudes (M6.5 - M7.6), the average of Campbell and Boore-Joyner fault distances, (11.1-26.4 km), site class (C and D) are shown in table 2. The references and definitions of 25 IMs seismic parameters are presented in Table 3, which are used in this study. These parameters are determined by Seism Signal 2018 software (2018).

Table 1 Near-source earthquake records

NO	Event	Year	Station Name	M	Component	PGA (g)
1	Imperial_Valley-06	1979	El_Centro_Array_#6	6.5	140	0.41
					230	0.44
2	Imperial_Valley-06	1979	El_Centro_Array_#7	6.5	140	0.34
					230	0.46
3	Irpinia-Italy-01	1980	Sturno	6.9	0	0.25
					270	0.36
4	Superstition Hills-02	1987	Parachute Test Site	6.5	225	0.46
					315	0.38
5	Loma Prieta	1989	Saratoga Aloha	6.9	0	0.51
					90	0.32
6	Erzincan, Turkey	1992	Erzincan	6.7	EW	0.50
					NS	0.52
7	Cape Mendocino	1992	Petrolia	7	0	0.59
					90	0.66

8	Landers	1992	Lucerne	7.3	260 345	0.73 0.79
9	Northridge-01	1994	Rinaldi Receiving Sta	6.7	228 318	0.83 0.49
10	Northridge-01	1994	Sylmar-Olive View	6.7	90 360	0.60 0.84
11	Kocaeli, Turkey	1999	Izmit	7.5	90 180	0.22 0.15
12	Chi-Chi Taiwan	1999	TCU065	7.6	E N	0.81 0.60
13	Chi-Chi, Taiwan	1999	TCU102	7.6	E N	0.30 0.17
14	Duzce, Turkey	1999	Duzce	7.1	180 270	0.35 0.54
15	Gazli, USSR	1976	Karakyr	6.8	0 90	0.61 0.72
16	Imperial Valley-06	1979	NO	6.5	140 230	0.59 0.78
17	Imperial Valley-06	1979	Chihuahua	6.5	012 282	0.27 0.25
18	Nahanni, Canada	1985	Site 1	6.8	10 280	0.98 1.10
19	Nahanni, Canada	1985	Site 2	6.8	240 330	0.49 0.32
20	Loma Prieta	1989	BRAN	6.9	0 90	0.48 0.53
21	Loma Prieta	1989	Corralitos	6.9	0 90	0.64 0.48
22	Cape Mendocino	1992	Cape Mendocino	7	0 90	1.50 1.04
23	Northridge-01	1994	LA-Sepulveda VA	6.7	270 360	0.75 0.93
24	Northridge-01	1994	Northridge-Saticoy	6.7	90 180	0.37 0.48
25	Kocaeli-Turkey	1999	Yarimca	7.5	60 330	0.27 0.35
26	Chi-Chi, Taiwan	1999	TCU067	7.6	E N	0.50 0.33
27	Chi-Chi, Taiwan	1999	TCU084	7.6	E N	1.16 0.42

Table 2 Far-source earthquake records

NO	Event	Year	Station Name	M	Component	PGA (g)
1	Northridge	1994	Beverly Hills-Mulhol	6.7	9 279	0.27 0.34
2	Northridge	1994	Canyon Country-WLC	6.7	0 270	0.34 0.40
3	Duzce, Turkey	1999	Bolu	7.1	0 90	0.46 0.52
4	Hector Mine	1999	Hector	7.1	0 90	0.29 0.37
5	Imperial Valley	1979	Delta	6.5	262 352	0.31 0.46
6	Imperial Valley	1979	El Centro Array #11	6.5	140 230	0.37 0.37
7	Kobe, Japan	1995	Nishi-Akashi	6.9	0 90	0.53 0.52
8	Kobe, Japan	1995	Shin-Osaka	6.9	0 90	0.52 0.23
9	Kocaeli, Turkey	1999	Duzce	7.5	180 270	0.22 0.25
10	Kocaeli, Turkey	1999	Arcelik	7.5	0 90	0.30 0.20
11	Landers	1992	Yermo Fire	7.3	270 360	0.24 0.15
12	Landers	1992	Cool water	7.3	LN	0.33

					TR	0.48
13	Loma Prieta	1989	Capitola	6.9	0 90	0.58 0.48
14	Loma Prieta	1989	Gilroy Array #3	6.9	0 90	0.49 0.32
15	Manjil, Iran	1990	Abbar	7.4	L T	0.41 0.39
16	Superstition Hills	1987	El Centro Imp. Co.	6.5	0 90	0.31 0.23
17	Superstition Hills	1987	Poe Road (temp)	6.5	270 360	0.52 0.35
18	Cape Mendocino	1992	Rio Dell Overpass	7.0	270 360	0.32 0.45
19	Chi-Chi, Taiwan	1999	CHY101	7.6	E N	0.15 0.18
20	Chi-Chi, Taiwan	1999	TCU045	7.6	E N	0.46 0.49
21	San Fernando	1971	LA - Hollywood Stor	6.6	90 180	0.44 0.37
22	Friuli, Italy	1976	Tolmezzo	6.5	0 270	0.51 0.45

Table 3 The intensity measure parameters (IMs) of ground motions

NO	Intensity measure parameters	Formulation	Reference
1	Peak ground acceleration (PGA)	$PGA = max\lvert a(t)\rvert$	-
2	Peak ground velocity (PGV)	$PGV = max\lvert v(t)\rvert$	-
3	Peak ground displacement (PGD)	$PGD = max\lvert d(t)\rvert$	-
4	PGA/PGV ratio	-	Naumoski, 1988
5	Root-Mean-Square of Acceleration RMS (g)	$a_{rms} = \sqrt{\frac{1}{t_d}\int_0^{td} a(t)^2\,dt}$	Dobry R., 1978
6	Root-Mean-Square of velocity RMS (cm)	$v_{rms} = \sqrt{\frac{1}{t_d}\int_0^{td} v(t)^2\,dt}$	Kramer SL., 1996
7	Root-Mean-Square of velocity RMS (cm)	$d_{rms} = \sqrt{\frac{1}{t_d}\int_0^{td} d(t)^2\,dt}$	Kramer SL., 1996
8	Arias density (I_a)	$I_a = \frac{\pi}{2g}\int_0^{td} a(t)^2\,dt$	Arias, 1970
9	Characteristic intensity (I_c)	$I_C = (a_{rms})^{2/3}\sqrt{t_d}$	
10	Specific energy density (SED)	$SED = \int_0^{td} v(t)^2\,dt$	
11	The cumulative absolute velocity (CAV)	$CAV = \int_0^{td} a(t)\,dt$	EPRI, 1988
12	Acceleration spectrum intensity: (ASI)	$ASI = \int_{0.1}^{0.5} S_a(\varepsilon = 0.05, t)\,dt$	Von Thun et al., 1988
13	Velocity spectrum intensity (VSI)	$VSI = \int_{0.1}^{2.5} S_v(\varepsilon = 0.05, t)\,dt$	Von Thun et al., 1988
14	Housner intensity (HI)	$HI = \int_{0.1}^{2.5} PS_v(\varepsilon = 0.05, t)\,dt$	Housner, 1952
15	Sustained maximum acceleration (SMA): (g)	The third highest absolute value of acceleration/velocity in the time-history	Nuttli, 1979
16	Sustained maximum velocity (SMV): cm/sec		Nuttli, 1979
17	Effective peak acceleration (EPA)	$EPA = \frac{mean\,(S_a^{0.1-0.5}(\varepsilon = 0.05))}{V}$	
18	A_{95} parameter	The level of acceleration that has up to 95% of the arias intensity	Sarma and Yang, 1987
19	The predominant period (T_P)	The period in which the greatest spectral acceleration occurs in the response spectrum acceleration calculated at 5% damping.	Miranda, 1993
20	The mean period (T_m)	$T_m = \frac{\sum C_i^2/f_i}{\sum C_i^2}$	Rathje *et al.*, 1998
21	Max. incremental velocity (MIV)	The maximum area under the acceleration curves between two zero crossings of the accelerogram.	Anderson and Bertero, 1987 and Guaman, 2010

22	The damage index (DI)	$DI = \frac{C}{2} \cdot \sum_{i=1}^{2n} u_i^c$	Malhotra, 2002
23	The number of effective cycles (N_{cy})	$N_{cy} = \frac{1}{2} \cdot \sum_{i=1}^{2n} \left(\frac{u_i}{u_{max}}\right)^2$	Malhotra, 2002
24	The impulsivity index (IP)	$IP = \frac{Ld_v}{V}$	Panella et al., 2017
25	The average spectral acceleration (Sa_{avg})	The geometric mean of the spectral acceleration ordinates a specified number of periods of 5% damping	Bianchini et al., 2009

3.0 CHARACTERISTICS OF MOMENT-RESISTING STEEL FRAMES

The correlation between the ground motions IMs parameters with structural response parameters was measured using 3-, 6- and 12-story MRSFs. These frames are designed with PGAs equal to 0.125g according to the seismicity region of these frames which are located in Alexandria, Egypt. The design spectrum of soil type "C" for dense or medium dense sand soil was used. In all structures, the floor plan has 3-bays with 8.0 m in each direction; the first story height is 4.6 m and 3.6 m for the upper stories, as shown in Figure 1 to Figure 4. The dead and live loads on all floors are 5 KPa and 2.5 KPa, respectively. These frames are designed according to ECP-201 (2012) and ECP-205 (2008) for strong column-weak beam requirements with ductility reduction factor and drift ratio equal to 7 and 0.75%, respectively. Wide flange Wide sections of steel members are selected from the ASTM (1985) with yield stress and modulus of elasticity of steel equal to 345 MPa and 200 GPa, respectively. The strain hardening ratio is equal to 1%. The exterior columns sizes are not the same as the sizes of the interior column at every floor level. Beams have the same section on the same floor level. The rigid connections between beam and columns are taken for all buildings. Panel zone strength, lateral-torsional buckling strength, slenderness ratios, and other design code requests for members have been applied. The details of cross-sections of the 3-, 6- and 12-story MRSFs are summarized in Table 4.

The Drain-2dx program (1992) is used in the analysis of the three frames under nonlinear time history analysis. 49 acceleration records of near- and far-source ground motion records identified by FEMA P695 (2009) without scaling are used in this study. The beams and columns of frames are modeled using the fiber beam-column element (type 15). This element is divided into segments without presenting further degrees of freedom and then each segment is divided into fibers. For each fiber, the stress-strain curve for concrete and steel type should be defined. Also, the shape function of the element is changed with changing the state of these elements without adding extra nodes or elements as indicated by Prakash and Powell (1992). The 3% viscous damping was taken in the first two natural modes of these frames.

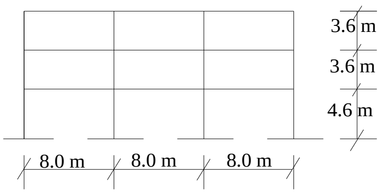

Figure 1 Elevation of the 3-story MRSF

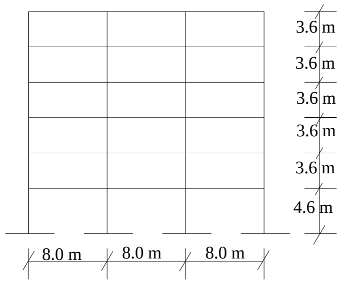

Figure 2 Elevation of the 6-story MRSF

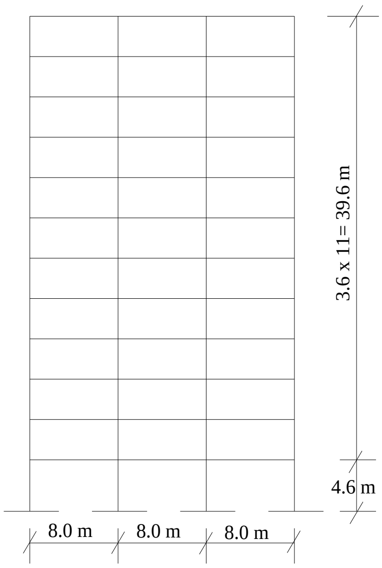

Figure 3 Elevation of the 12-story MRSF

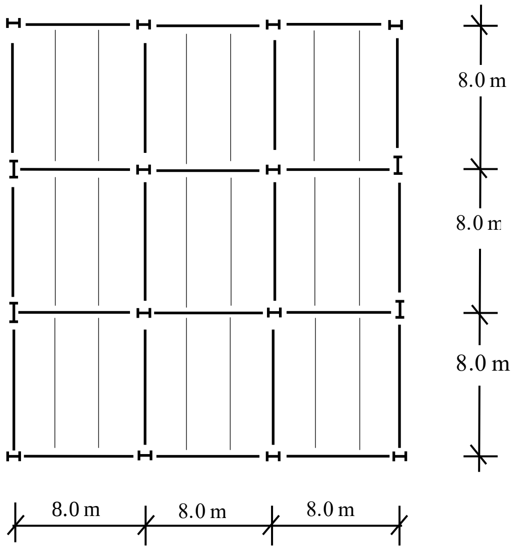

Figure 4 Plan of the three buildings

Table 4 Cross-section details of the 3-, 6- and 12-story MRSFs.

3-story				12-story			
Story	Beams	Exterior column	Interior column	Story	Beams	Exterior column	Interior column
1	W21x50	W14x61	W14x109	1	W30x108	W14x257	W14x311
2	W18x40	W14x38	W14x109	2	W30x108	W14x193	W14x311
3	W18x35	W14x53	W14x109	3	W30x 99	W14x193	W14x257
6-story				4	W30x 99	W14x145	W14x257
Story	Beam	Exterior column	Interior column	5	W30x 90	W14x145	W14x233
				6	W30x 90	W14x132	W14x233
1	W24x 68	W14x109	W14x176	7	W27x 84	W14x120	W14x211
2	W24x 68	W14x82	W14x176	8	W24x 84	W14x109	W14x193
3	W21x 62	W14x82	W14x132	9	W24x 76	W14x109	W14x159
4	W21x 55	W14x61	W14x132	10	W21x 62	W14x 74	W14x145
5	W21x 44	W14x53	W14x82	11	W21x 44	W14x 53	W14x109
6	W16x 31	W14x43	W14x82	12	W18x 35	W14x 53	W14x109

4.0 INTENSITY MEASURES VERSUS STRUCTURAL RESPONSE CORRELATION

The correlation between the ground motion IMs and the structure performance parameters are computed with the Pearson correlation coefficient as:

$$\rho = \frac{\sum_{i=1}^{N}(X_i-\bar{X})(Y_i-\bar{Y})}{\sqrt{\sum_{i=1}^{N}(X_i-\bar{X})^2\sum_{i=1}^{N}(Y_i-\bar{Y})^2}} \quad (1)$$

In which $\bar{X}$ and $\bar{Y}$ are the mean values of X_i and Y_i respectively, and N is the number of pairs of values (X_i, Y_i) in the data. The range of this factor is between -1 and 1. Nonlinear time history analysis for 3-, 6- and 12-story MRSFs are performed under near- and far-source ground motion records identified by FEMA P695 [9]. After that, the regression analyses are used to present the correlation between structural response parameters and IMs parameters through the following sections.

4.1 Correlation Between Structural Response Parameters

The Pearson correlation coefficients between structural response parameters for 3-, 6- and 12-story MRSFs are determined as indicated in Table 5. For near-source records, the correlation between MSDR and RDR is a moderate correlation with SF in 3- and 6-story frames and strong correlation in the 12-story frame. By far-source records, the correlation between the MSDR and RDR is a strong correlation with SF in all frames. Also, the correlation between the MSDR and RDR is strong in all frames for both near-and far-source earthquakes. This outcome can be referring to the fact that both MSDR and RDR are established based on the displacement requirement.

Table 5 Correlation coefficients among structural response parameters

Frames		*Near-source*			*Far-source*		
		SF	RDR	MSDR	SF	RDR	MSDR
3-story	SF	1.00			1.00		
	RDR	0.63	1.00		0.89	1.00	
	MSDR	0.63	0.99	1.00	0.90	0.98	1.00
6-story	SF	1.00			1.00		
	RDR	0.60	1.00		0.81	1.00	
	MSDR	0.56	0.92	1.00	0.73	0.77	1.00
12-story	SF	1.00			1.00		
	RDR	0.86	1.00		0.76	1.00	
	MSDR	0.75	0.74	1.00	0.46	0.51	1.00

4.2 Correlation Between Earthquake Intensity Measures And Structural Response

Figure 5 presents the absolute values of correlation coefficients between the MSDR and IMs of near- and far-source earthquakes in the 3-story MRSF. In near-source earthquakes, MIV has the best correlation with MSDR, followed by PGV, V_{rms}, HI, VSI, and Sa_{avg}; whereas the weakest correlated IMs are DI, T_p, SMA, N_{cy}, CAV, and I_a. By far-source earthquakes, VSI and HI are the strongest correlated parameters, followed by Sa_{avg}, MIV, PGV, and a_{rms}; whereas the remnant IMs parameters are weakest correlated with MSDR. Also, it can be seen that the highest correlation coefficients between the MSDR and most of seismic IMs parameters by far-source records that are more than near-source records.

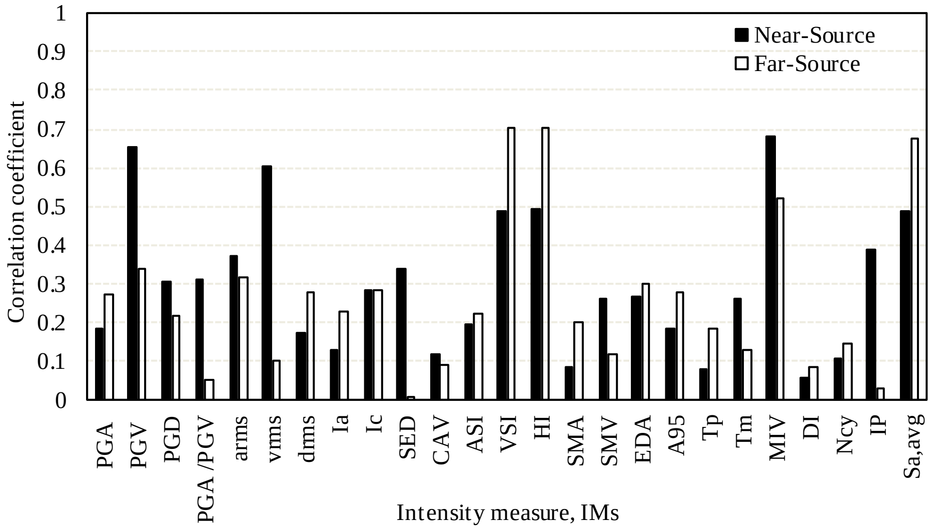

Figure 5 Correlation coefficients between MSDR and IMs of near-and far-source for the 3-story MRSF

Figure 6 presents the absolute values of correlation coefficients between the RDR and IMs of near- and far-source earthquakes in the 3-story MRSF. In near-source earthquakes, MIV has the best correlation with RDR, followed by PGV and V_{rms}. Meanwhile, the poor correlation IMs are DI, SMA, T_p, CAV, and I_a. By far-source earthquakes, HI has the best correlation with RDR, followed by VSI, Sa_{avg}, and MIV. Meanwhile, the lowest correlation IMs are PGA/PGV, I_p, SED, DI, and CAV. Also, it can be seen that the highest correlation coefficients between the RDR and most of seismic IMs parameters by near-source records that are more than far-source records.

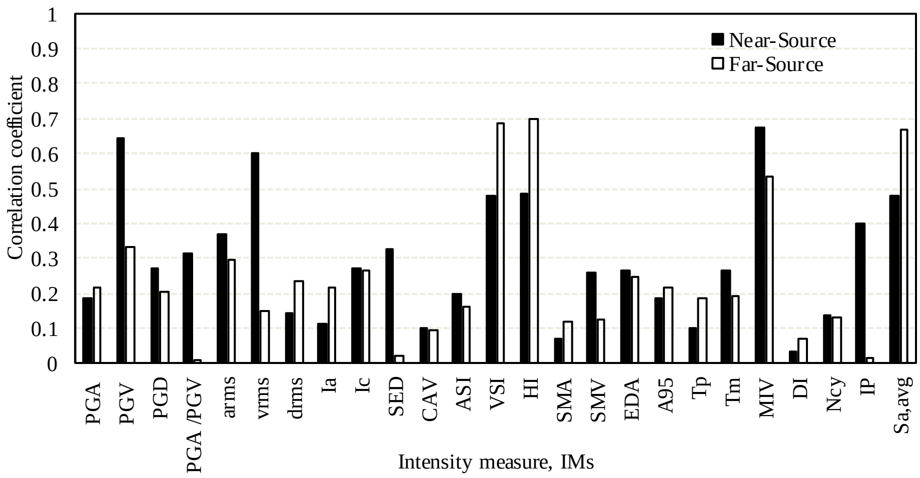

Figure 6 Correlation coefficients between RDR and IM of near-and far-source for the 3-story MRSF

Figure 7 presents the absolute values of correlation coefficients between, the SF and IMs of near- and far-source earthquakes in the 3-story MRSF. In near-source earthquakes, the correlation between the SF and the ground motion IMs parameters are weak correlations. While in far-source earthquakes, HI has the best correlation with SF, followed by VSI and Sa_{avg}; whereas the remnant IMs parameters are the weakest correlated with SF. Also, the highest correlation coefficients between the SF and most of seismic IMs parameters by near-source records are more than those by far-source records.

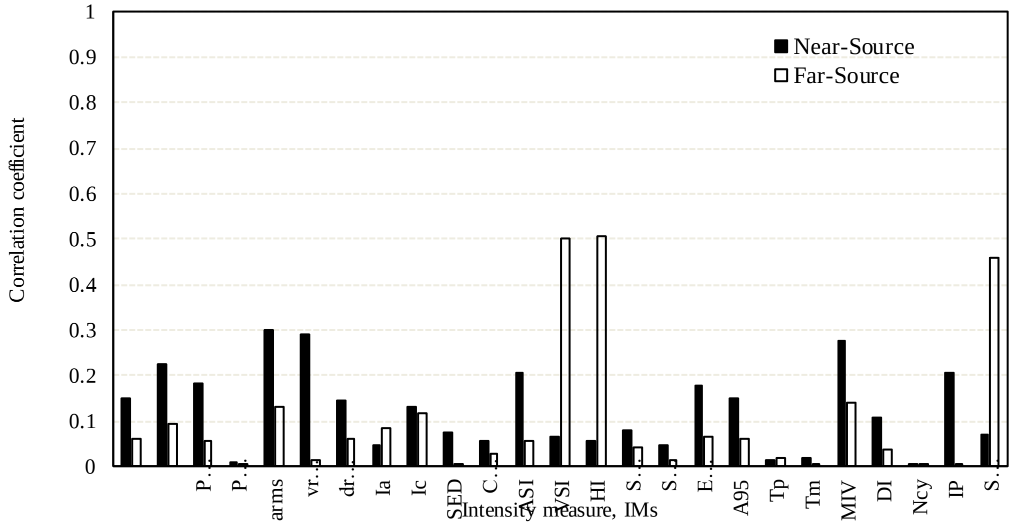

Figure 7 Correlation coefficients between SF and IMs of near- and far-source for the 3-story MRSF

Figure 8 presents the absolute values of correlation coefficients between the MSDR and ground motions IMs parameters of near- and far-source earthquakes for the 6-story MRSF. In near-source earthquakes, MIV has the best correlation with MSDR, followed by PGV, V_{rms}, HI, and Ip; whereas the weakest correlated IMs are SMA, Ia, d_{rms}, DI, CAV, and PGA. By far-source earthquakes, Sa_{avg}, HI, and VSI are the strongest correlated parameters; whereas the weakest correlated IMs are Tm, Ncy, PGA/PGV, V_{rms}, and SED. Also, it can be seen that the highest correlation coefficients between the MSDR and most of seismic IMs parameters by far-source records that are more than near-source records.

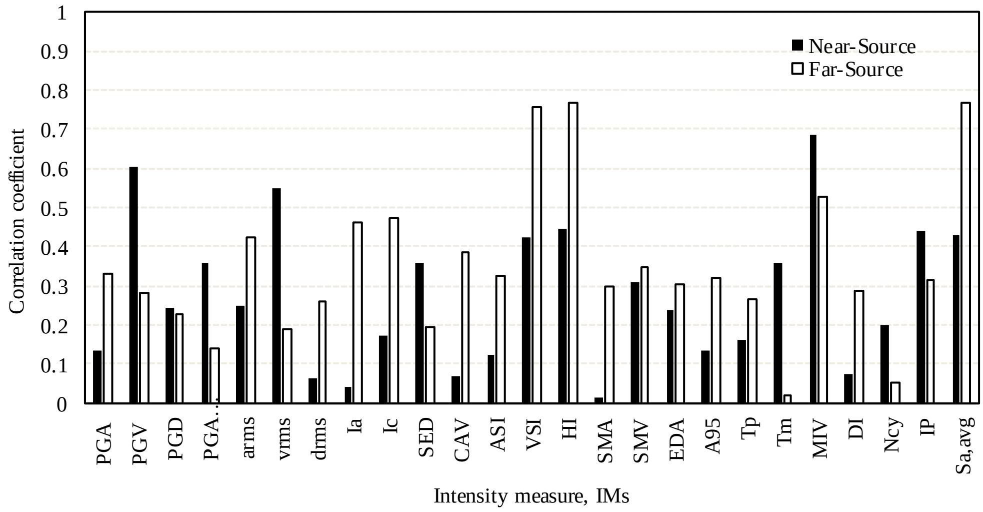

Figure 8 Correlation coefficients between MSDR and IMs of near- and far-source for the 6-story MRSF

Figure 9 presents the absolute values of correlation coefficients between the RDR and IMs of near- and far-source earthquakes for the 6-story MRSF. In near-source earthquakes, V_{rms} has the best-correlated parameter, followed by MIV, PGV, and IP. Meanwhile, the poor correlation IMs are I_a, PGA, I_c, CAV, ASI, SMA, and A_{95}. By far-source earthquakes, HI and Sa_{avg} are the strongest correlated parameters, followed by VSI and CAV. Meanwhile, the lowest correlation IMs are EDA, PGA, ASI, PGD, and d_{rms}. Also, it can be seen that the highest correlation coefficients between the RDR and most of the seismic IMs parameters by near-source records that are more than far-source records.

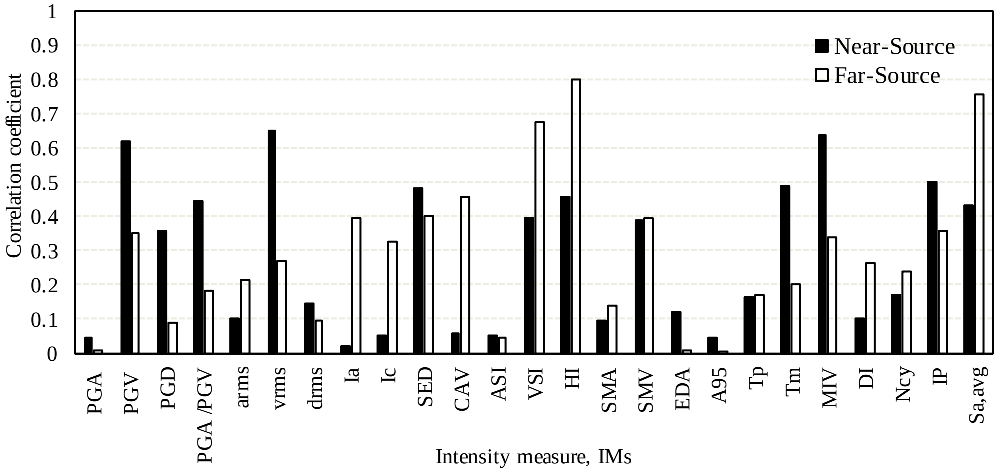

Figure 9 Correlation coefficients between RDR and IM of near- and far-source for the 6-story MRSF

Figure 10 presents the absolute values of correlation coefficients between, the SF and IMs of near- and far-source earthquakes for the 6-story MRSF. In near-source earthquakes, the correlation between the SF and the ground motion IMs parameters are weak correlations except for the IP parameter. By far-source earthquakes, HI is the strongest correlated parameter followed by Sa_{avg}, VSI, SMV, and Ia; whereas the remnant IMs parameters are the weakest correlated with SF. Also, it can be seen that the highest correlation coefficients between the SF and most of seismic IMs parameters by far-source records are more than those in near-source records.

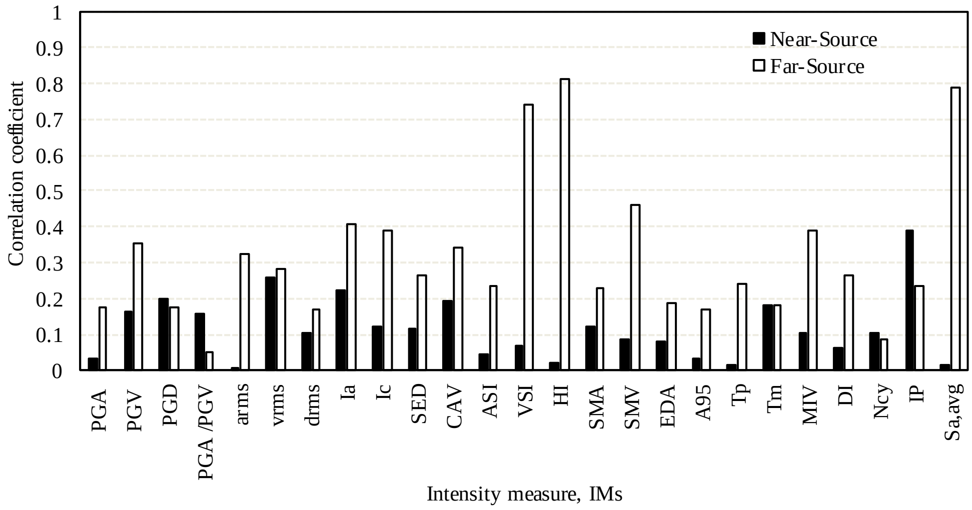

Figure 10 Correlation coefficients between SF and IM of near- and far-source for the 6-story MRSF.

Figure 11 presents the absolute values of Pearson correlation coefficients between the MSDR and IMs of near- and far-source earthquakes in the 12-story MRSF. In near-source earthquakes, MIV has the best correlation with MSDR, followed by PGV, IP, and V_{rms}; whereas the weakest correlated IMs are d_{rms}, CAV, DI, PGA, and I_a. By far-source earthquakes, Sa_{avg} is the strongest correlated parameters followed by HI, VSI, and MIV; whereas the weakest correlated IMs parameters are N_{cy}, Tm, PGA/PGV, and SED. Also, it can be seen that the highest correlation coefficients between the MSDR and most of seismic IMs parameters by far-source records are more than those in near-source records.

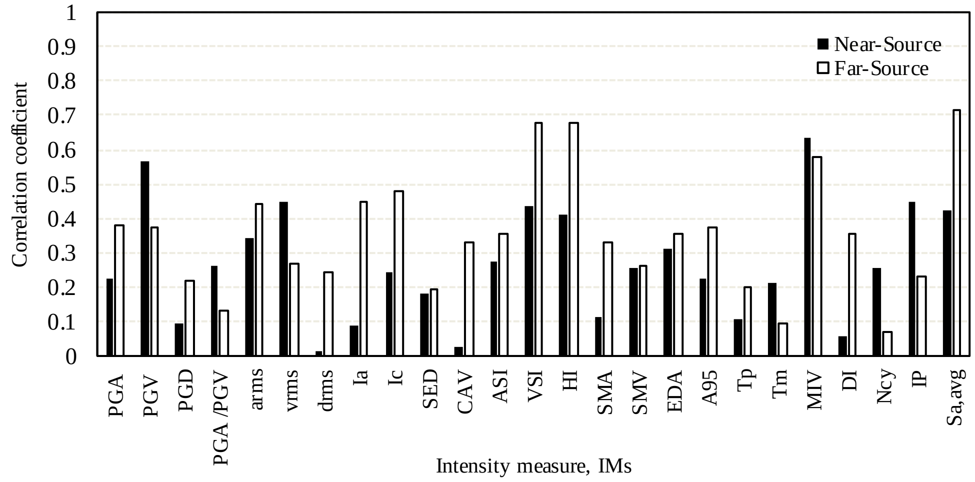

Figure 11 Correlation coefficients between MSDR and IMs of near-and far-source for the 12-story MRSF

Figure 12 presents the absolute values of correlation coefficients between the RDR and IMs of near- and far-source earthquakes in the 12-story MRSF. In near-source earthquakes, V_{rms} has the best-correlated parameter, followed by MIV, PGV, T_m, and I_P. Meanwhile, the poor correlation IMs are PGA, A_{95}, I_c, ASI, I_a, CAV, arms, and EDA. By far-source earthquakes, Sa_{avg} is the strongest correlated parameters, followed by HI, VSI, and MIV. Meanwhile, the lowest correlation IMs are N_{cy}, T_m, PGA/PGV, and SED. Also, it can be seen that the highest correlation coefficients between the RDR and most of seismic IMs parameters by far-source records that are more than near-source records.

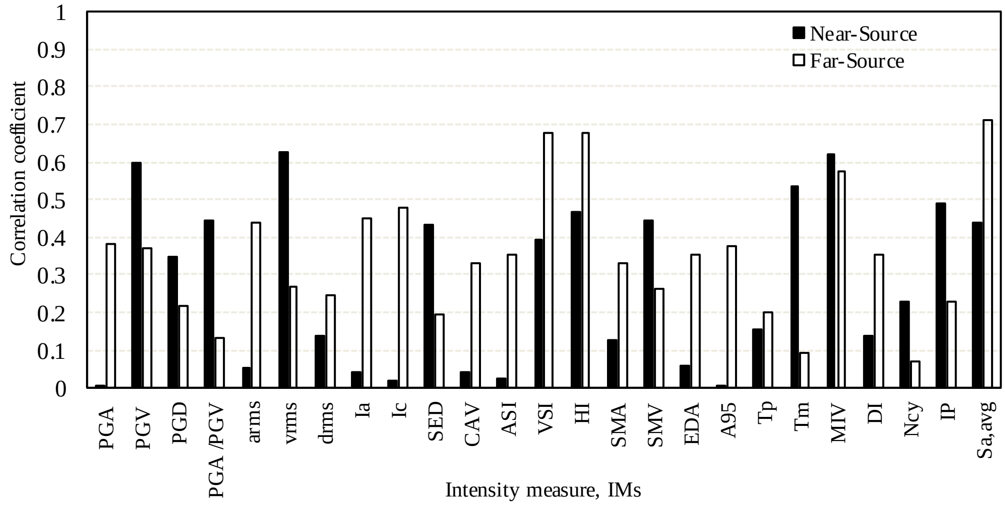

Figure 12 Correlation coefficients between RDR and IM of near- and far-source for the 12-story MRSF

Figure 13 presents the absolute values of correlation coefficients between, the SF and IMs of near- and far-source earthquakes in the 12-story MRSF. In near-source earthquakes, IP has the best-correlated parameter, followed by V_{rms}, PGV, MIV, T_m, and PGA/PGV. The remnant IMs parameters are the weakest correlated parameters with SF. By far-source earthquakes, Sa_{avg} has the best correlation with SF, followed by HI and VSI; whereas the remnant IMs parameters are weakest correlated with SF. Also, it can be seen that the highest correlation coefficients between, the SF and most of seismic IMs parameters by near-source records are more than those in far-source records.

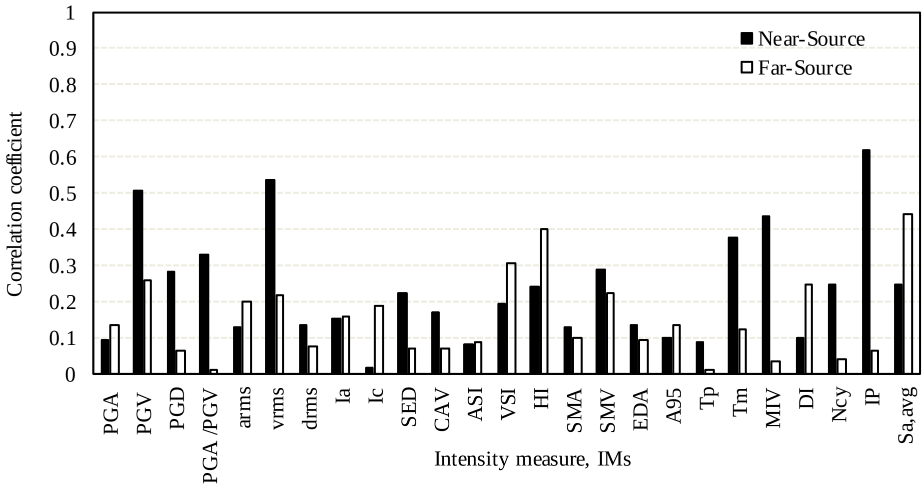

Figure 13 Correlation coefficients between SF and IM of near- and far-source for the 12-story MRSF

Table 6 Correlation coefficients between IMs and structural response parameter of 3-story MRSF

IMS	NEAR-SOURCE			FAR-SOURCE		
	MSDR	RDR	SF	MSDR	RDR	SF
PGA	0.185	0.183	0.151	0.275	0.215	0.248
PGV	0.652	0.641	0.225	0.339	0.333	0.306
PGD	0.304	0.268	0.183	-0.219	-0.204	-0.231
PGA /PGV	-0.314	-0.313	-0.010	0.050	-0.007	0.037
A_{RMS}	0.374	0.366	0.299	0.315	0.296	0.358
V_{RMS}	0.606	0.598	0.292	0.103	0.149	0.117
D_{RMS}	0.171	0.141	0.143	-0.279	-0.233	-0.248
IA	0.129	0.115	-0.048	0.230	0.217	0.289
IC	0.281	0.268	0.133	0.284	0.264	0.340
SED	0.338	0.328	0.075	-0.006	0.023	0.017
CAV	0.119	0.100	-0.057	0.088	0.094	0.169
ASI	0.197	0.198	0.205	0.225	0.159	0.237
VSI	0.485	0.479	0.063	0.703	0.688	0.709
HI	0.493	0.484	0.055	0.702	0.697	0.713
SMA	0.083	0.070	0.078	0.201	0.121	0.200
SMV	0.264	0.257	0.047	0.117	0.122	0.125
EDA	0.267	0.265	0.177	0.301	0.247	0.255
A_{95}	0.186	0.184	0.151	0.275	0.215	0.247
T_p	0.079	0.102	-0.015	0.186	0.186	0.132
T_m	0.262	0.264	-0.018	0.127	0.190	0.037
MIV	0.683	0.677	0.274	0.520	0.534	0.372
DI	0.055	0.031	0.107	0.087	0.069	0.189
N_{cy}	-0.109	-0.139	-0.004	-0.143	-0.132	-0.022
IP	-0.386	-0.398	-0.208	-0.029	-0.016	0.041
Sa_{avg}	0.487	0.482	0.068	0.678	0.670	0.677

Table 7 Correlation coefficients between IMs and structural response parameter of 6-story MRSF

IMs	Near-Source			Far-Source		
	MSDR	RDR	SF	MSDR	RDR	SF
PGA	0.132	0.048	0.031	0.329	0.011	0.175
PGV	0.604	0.623	0.165	0.280	0.355	0.354
PGD	0.242	0.360	0.197	-0.230	-0.088	-0.178
PGA /PGV	-0.357	-0.446	-0.155	0.140	-0.185	-0.049
a_{rms}	0.251	0.102	0.005	0.424	0.212	0.324
v_{rms}	0.549	0.649	0.260	0.188	0.270	0.284
d_{rms}	0.065	0.147	0.101	-0.262	-0.099	-0.167
Ia	0.045	-0.023	-0.222	0.462	0.396	0.408
Ic	0.171	0.050	-0.123	0.471	0.330	0.389
SED	0.359	0.481	0.114	0.193	0.401	0.265
CAV	0.067	0.058	-0.192	0.387	0.461	0.343

ASI	0.126	-0.054	0.042	0.325	0.045	0.235
VSI	0.426	0.395	-0.066	0.755	0.677	0.740
HI	0.445	0.459	-0.022	0.768	0.798	0.810
SMA	0.017	-0.096	-0.121	0.296	0.140	0.231
SMV	0.307	0.390	0.085	0.349	0.397	0.458
EDA	0.238	0.120	0.078	0.306	-0.011	0.189
A_{95}	0.133	0.049	0.032	0.321	-0.003	0.167
T_p	0.165	0.166	-0.014	0.268	0.171	0.241
T_m	0.359	0.488	0.180	0.021	0.201	0.182
MIV	0.683	0.641	0.104	0.528	0.339	0.392
DI	-0.073	-0.102	-0.060	0.287	0.266	0.263
N_{cy}	-0.199	-0.172	-0.102	0.052	0.240	0.084
IP	-0.443	-0.500	-0.387	0.316	0.359	0.237
Sa_{avg}	0.428	0.434	-0.015	0.770	0.760	0.789

Table 8 Correlation coefficients between IMs and structural response parameter of 12-story MRSF

IMs	Near-Source			Far-Source		
	MSDR	RDR	SF	MSDR	RDR	SF
PGA	0.226	0.002	0.095	0.380	-0.082	0.138
PGV	0.567	0.597	0.509	0.373	0.231	0.261
PGD	0.093	0.347	0.282	-0.218	0.013	-0.063
PGA /PGV	-0.261	-0.443	-0.327	0.132	-0.225	-0.009
a_{rms}	0.343	0.056	0.129	0.441	0.179	0.201
v_{rms}	0.446	0.626	0.535	0.269	0.370	0.218
d_{rms}	-0.017	0.139	0.133	-0.245	0.020	-0.074
Ia	0.087	-0.044	-0.153	0.450	0.318	0.160
Ic	0.244	0.019	-0.016	0.480	0.265	0.186
SED	0.184	0.436	0.226	0.195	0.397	0.071
CAV	0.025	0.043	-0.171	0.331	0.412	0.068
ASI	0.274	-0.025	0.084	0.352	-0.062	0.089
VSI	0.434	0.391	0.193	0.676	0.355	0.305
HI	0.414	0.470	0.243	0.679	0.533	0.402
SMA	0.113	-0.125	-0.131	0.331	0.022	0.100
SMV	0.258	0.445	0.291	0.265	0.277	0.226
EDA	0.311	0.056	0.138	0.354	-0.096	0.095
A_{95}	0.227	0.003	0.098	0.375	-0.098	0.135
T_p	0.108	0.155	0.091	0.203	0.006	-0.011
T_m	0.214	0.535	0.375	0.094	0.236	0.125
MIV	0.638	0.623	0.438	0.577	0.042	0.032
DI	-0.059	-0.140	-0.101	0.354	0.370	0.245
N_{cy}	-0.258	-0.226	-0.248	0.072	0.383	0.042
IP	-0.450	-0.492	-0.622	0.231	0.322	-0.063
Sa_{avg}	0.423	0.442	0.247	0.713	0.563	0.444

Tables 6, Table7, and Table 8 present the Pearson correlation coefficients between the structural response parameter and IMs of near- and far-source earthquakes in the 3-, 6- and 12-story MRSFs. Based on the observation of these tables; it can be found that in general, the MSDR is the best-correlated parameter with most of seismic IMs parameters than RDR and SF. Also, SF is the weakest correlated parameter with most of seismic IMs parameters. These results are consistent with the results obtained by Jayaram (2010).

Also, among all of the MRSFs, the correlation values of MSDR parameters with MIV are the highest range of the correlation value with 6-story MRSF. While in far-source, the correlation value of MSDR parameters with Sa_{avg} is the highest range of correlation values with 6-story MRSF. Also, among all of the MRSFs, the correlation between RDR and MIV is the highest range of the correlation value with 3-story MRSF. While in far-source, the correlation values of MSDR parameters with HI is the highest range of the correlation value with 6-story MRSF. Also, among all of the MRSFs, the correlation values of SF parameters with IP are the highest range of correlation values with 12-story MRSF. While in far-source, the correlation values of MSDR parameters with Sa, avg is the highest range of correlation values with 6-story MRSF. Also, among all of the MRSFs, the MIV parameter is considered as the highest correlated IMs parameters of near- and far-source earthquakes with MSDR. While, the poorly correlated ground motion IMs parameters are N_{cy}, T_p, and d_{rms}.

In the three MRSFs, there is not much difference in Pearson coefficients between the structural response parameters and IMs of near- and far-source earthquakes. Thus it can be concluded that the results aren't correlated to the frame heights and they can be advanced for all the MRSFs.

5.0 CONCLUSIONS

The present study has investigated the correlation between 25 IMs parameters of near- and far-source of earthquakes and the seismic response parameter of 3-, 6- and 12-story

MRSFs. The seismic response parameter was expressed in terms of the MSDR, RDR, and SF. Based on an estimation of the correlation coefficients, the following conclusions can be drawn:

The maximum story drift ratio appears to be a suitable engineering demand parameter to correlate with most of seismic IMs parameters compared to the roof drift ratio and the maximum base shear force.

1. The maximum base shear force is the weakest correlated parameter with most of seismic IMs parameters compared to the roof drift ratio and the maximum story drift ratio.
2. For near-source earthquakes, MIV, PGV, V_{rms}, HI, VSI, and Sa_{avg} are considered as the highest correlated IMs parameters with both MSDR and RDR.
3. For far-source earthquakes, Sa_{avg}, HI, VSI, and MIV are considered as the highest correlated IMs parameters with both MSDR and RDR.
4. In both near- and far-source earthquakes, the maximum incremental velocity (MIV) parameter is considered as the highest correlated IMs parameters with MSDR. Also, the number of effective cycles (N_{cy}) is considered as the weakest correlated IMs parameters.
5. The correlation between the structural response parameters and IMs of near- and far-source earthquakes are not correlated to the frame heights.
6. The results of the analysis provide suitable evidence on how intensity measure parameters of ground motion earthquakes and structural response affect the safety levels of seismic design of buildings.

References

[1] Anderson, J.C., and Bertero, V.V. 1987. Uncertainties in Establishing Design Earthquakes. *Journal of Structural Engineering* 113: 1709.

[2] Ang, A.H.S., and Tang, W.H. 2007. Probability Concepts in Engineering: Emphasis on Applications in Civil & Environmental Engineering. 1, Wiley, and Sons.

[3] Arias, A. 1970 A measure of earthquake intensity, in Seismic Design for Nuclear Power Plants. R.J. Hansen (Editor). 438–483. MIT Press, Cambridge, Massachusetts:

[4] ASTM. 1985. Cycle counting in fatigue analysis, Annual Book of ASTM Standards. 03.01, Designation E1049-85.

[5] Bianchini, M., Diotallevi, P., and Baker, J.W. 2009. Prediction of Inelastic Structural Response Using an Average of Spectral Accelerations. 10th International Conference on Structural Safety and Reliability (ICOSSAR09), Osaka, Japan.

[6] Dobry, R., Idriss, I.M., NgE. 1978. Duration characteristics of horizontal components of strong-motion earthquake records. Bull Seismol. Soc, Am. 68:1487–520.

[7] ECP-201. 2012. Egyptian Code for Calculating Loads and Forces in Structural Work and Masonry. National Research Center for Housing and Building, Giza, Egypt

[8] ECP-205. 2008. Egyptian Code Of Practice For Steel Construction And Bridges : (Allowable Stress Design). Ministry of Housing and Utilities and Urban Development.

[9] EPRI. 1988. A Criterion for determining exceedance of the operating basis earthquake. In: Electric Power Research Institute, Palo Alto, CA, prepared by Jack R. Benjamin and Associates Inc, Report No: NP-5930

[10] Esfahanian, A., and Aghakouchak, A.A. 2020. Sensitivity analysis of the influence of ground motion intensity levels on the seismic behavior of steel frames in the assessment of the target displacement considering near-fault effects. *Canadian Journal of Civil Engineering* 47: 470-486.

[11] FEMA P695. 2009. Quantification of building seismic performance factors. FEMA, Prepared by the Applied Technology Council for the Federal Emergency Management Agency, Washington, D.C.

[12] Fontara, K.M. Athanatopoulou, A.M. and Avramidis, I.E. 2012. Correlation between Advanced, Structure-Specific Ground Motion Intensity Measures, and Damage Indices. 15th World Conference on Earthquake Engineering, Lisbon, Portugal, 1

[13] Guaman, J.W. 2010. Empirical Ground Motion Relationship for Maximum Incremental Velocity. Master's Thesis, University of Notre Dame.

[14] Hancock, J., Bommer, J.J., and Stafford, P.J. 2008. Numbers of scaled and matched Accelerograms required for inelastic dynamic analyses. *Earthquake Engineering and Structural Dynamics* 37: 1585-1607.

[15] Habibi, A., and Jami, E. 2016. Correlation between Ground Motion Parameters and Target Displacement of Steel Structures. *International Journal of Civil Engineering* 15: 163–174.

[16] Housner, G.W. 1952. Spectrum Intensities of Strong-Motion Earthquakes. In: *Proceedings of the Symposium on Earthquake and Blast Effects on Structures*: Los Angeles. California, Earthquake Engineering Research Institute, Los Angeles. 20-36.

[17] Jayaram, N., Mollaioli, F., Bazzurro, P., De Sortis, A., and Bruno, S. 2010. Prediction of the structural response of reinforced concrete frames subjected to earthquake ground motions. 9th U.S. National and 10th Canadian Conference on Earthquake Engineering. 428-437, 25-29 July, Toronto, Canada.

[18] Kenari, M.S., and Celikag, M. 2019. Correlation of Ground Motion Intensity Measures and Seismic Damage Indices of Masonry-Infilled Steel Frames. *Arabian Journal for Science and Engineering* 44: 5131–5150.

[19] Kramer, S.L. 1996. *Geotechnical Earthquake Engineering*. NewJersy: Prentice Hall.

[20] Makris, N., and Black, J.C. 2004. Evaluation of Peak Ground Velocity as a "Good" Intensity Measure for Near Source Ground Motions. *Journal of Engineering Mechanics* 130: 1032-1044.

[21] Malhotra, P.K. 2002. Cyclic-demand spectrum. Earthquake Engineering and Structural Dynamics. 31: 1441–1457.

[22] Miranda, E. (1993). Evaluation of site-dependent inelastic seismic design spectra. Journal of Structural Engineering. 119: 1319–1339.

[23] Naumoski, N., Tso, W.K., and Heidebrecht, A.C. 1988. A selection of Representative Strong Ground Motion Earthquake Records Having Different A/V Ratios. Report No. EERG 88/01, Earthquake Engineering Research Group, McMaster University, Hamilton, Ontario.

[24] Nuttli, O.W. 1979. The relation of sustained maximum ground acceleration and velocity to earthquake intensity and magnitude. Miscellaneous Paper S-71-1, Report 16, U.S. Army Corps of Engineers, Waterways Experiment Station, Vicksburg, Mississippi.

[25] Perrault, M., and Guéguen, P. 2015. Correlation between Ground Motion and Building Response Using California Earthquake Records. *Earthquake Spectra* 31: 2027-2046.

[26] Pinzon, L.A., Vargas-Alzate, Y.F., Pujades, L.G., and Dia, S. 2020. A drift-correlated ground motion intensity measure: Application to steel frame buildings. *Soil Dynamics and Earthquake Engineering* 132: 106096.

[27] Prakash, V., and Powell, G.H. 1992. DRAIN-2DX user guide. Department of Civil Engineering, University of California, Berkeley, California.

[28] Panella, D.S., Tornello, M.E., and Frau, C. 2017. A simple and intuitive procedure to identify pulse-like ground motions. *Soil Dynamics and Earthquake Engineering* 94: 234-243.

[29] Rathje, E.M., Abrahamson, N.A., and Bray, J.D. 1998. Simplified frequency content estimates of earthquake ground motions. *Journal of Geotechnical and Geoenvironmental Engineering* 124: 150-159.

[30] Riddell, R. 2007. On ground motion intensity indices. *Earthquake Spectra* 23: 147-173.

[31] Sarma, S.K., and Yang, K.S. 1987. An evaluation of strong-motion records and a new parameter A95. Earthquake Engineering & Structural Dynamics, 15: 119 – 132. DOI: 10.1002/eqe.4290150109.

[32] SeismoSoft. 2013. SeismoSignal V.5.1.2—A computer program for processing and deriving properties of strong motion data. Retrieved from http://www.seismosoft.com. [Google Scholar]

[33] Shokrabadi, M., and Burton, H.V. (2017). Ground Motion Intensity Measures for Rocking Building Systems. *Earthquake Spectra* 33: 1533–1554.

[34] Von, Thun J.L., Rochim, L.H., Scott, G.A., and Wilson, J.A. 1988. Earthquake ground motions for design and analysis of dams. Earthquake Engineering and Soil Dynamics II - Recent Advances in Ground-Motion Evaluation, *Geotechnical Special Publication*. 20: 463-481.

[35] Yang, D., Pan, J., and Li, G. 2009. Non-structure-specific intensity measure parameters and characteristic period of near-fault ground motions. *Earthquake Engineering and Structural Dynamics*. 38: 1257–1280.